$\mathscr{R}$esearch Article

In vitro antioxidant, anti-inflammatory, anti-cancer and *in silico* molecular docking studies of *Clerodendrum thomsoniae*

Pallab Kar[1]*, Ayodeji O. Oriola[2]*, Adebola O. Oyedeji[1,2]

[1]African Medicinal Flora and Fauna Research Niche, Walter Sisulu University, Mthatha, South Africa, [2]Department of Chemical and Physical Sciences, Walter Sisulu University, Mthatha, South Africa

ABSTRACT

Clerodendrum thomsoniae is a member of the Lamiaceae family and is found throughout Asia, Australia, Africa, and America. *C. thomsoniae* (CT), mostly utilized in the floriculture sector, is sometimes referred to as bleeding heart vine or bag flower due to its exquisite decorative qualities. Apart from its high value in the floriculture industry, the plant has been utilized in traditional Indian and Japanese medicine to treat a variety of ailments. There is a dearth of information on the biological properties of the plant and its putative ingredients. Therefore, this study evaluated the antioxidant, anti-inflammatory, and anti-cancer potentials of the extract, as well as identified its phytocompounds. The antioxidant screening was based on nitric oxide (NO), hydrogen peroxide (H_2O_2), hydroxyl, and superoxide radical scavenging assays. *In vitro* anti-inflammatory activity of the extract was based on the egg albumin denaturation (EAD) assay, while the 3-(4,5-dimethylthiazolyl-2)-2,5-diphenyltetrazolium bromide (MTT) cell viability assay was used to determine its anti-cancer potential. The chemical composition of the extract was determined using the hyphenated gas chromatography-mass spectrometry (GC-MS) method. Lastly, the identified phytocompounds were molecular docked against the inflammatory [NF-κβ (4DN5)] and cancer [mdm2 (3W69)] proteins. At 200 μg/mL, CT extract-treated Vero normal cells exhibited more viability (78.32±1.19%) than the one treated with the human renal adenocarcinoma (ACHN) cell line (33.45±0.66%), which suggests CT extract to be selectively cytotoxic to the cancer cells. The extract also demonstrated considerable inhibition of EAD (IC_{50}=164.59±17.85 μg/mL). Thus, the observed anti-cancer and anti-inflammatory properties of CT extract may be attributed to its notable NO and H_2O_2 radicals scavenging activities, with IC_{50} values of 205.7±11.44 and 69.74±6.50 μg/mL respectively. GC-MS analysis of the extract revealed sixteen major compounds. *In silico* studies indicated α-tocopherol and stigmasterol as the most promising compounds, having exhibited the highest binding energy scores of -9.9 and -8.7 kcal/mol against NF-κβ (4DN5) and mdm[2] (3W69) proteins respectively. In conclusion, *C. thomsoniae* leaf extract showed considerable antioxidant, anti-inflammatory, and anti-cancer properties, which may be attributed to its α-tocopherol and stigmasterol contents.

KEYWORDS: *Clerodendrum thomsoniae*, Antioxidant, Anti-inflammatory, Anti-cancer, *In vitro* and *in silico* biological studies, α-Tocopherol, Stigmasterol

*Corresponding authors:
Pallab Kar
E-mail: pallabkar.bio@gmail.com
Ayodeji O. Oriola
E-mail: aoriola@wsu.ac.za

INTRODUCTION

The immune system uses free radical generation as a tactic to keep the body homeostasis so that invasive pathogens are eliminated (Chaplin, 2010). Free radical creation is a byproduct of cell metabolic activity. According to Wolfe *et al.* (2008), free radicals are extremely reactive molecules with unpaired electrons in their outer orbitals that have the capacity to exist on their own. Numerous immune cell types, especially phagocytes including dendritic cells, neutrophils, and macrophages, are crucial in eradicating sick and damaged cells by generating free radicals and triggering programmed

cell death (Hirayama *et al.*, 2017). However, reactive oxygen species (ROS) or free radicals such as superoxide anions, hydroxyl radicals, and hydrogen peroxide are produced if the amount of oxygen supply is excessive or its reduction is insufficient in the system (Kris-Etherton *et al.*, 2004). The reactive oxygen species (ROS) or reactive nitrogen species (RNS) are chemically very reactive molecules containing an unstable oxygen species having unpaired electrons with reactive chemical properties, along with different types of free radicals like H_2O_2 formed through any route in cells as a consequence of oxidative biochemical reactions (Kris-Etherton *et al.*, 2004). These free radicals have the ability to change components that

are important to biology, including proteins, carbohydrates, membrane lipids, DNA, and lipids, which can ultimately result in cellular malfunction or death (Phaniendra *et al.*, 2015). In addition to an endogenous source, some of the exogenous factors contributing to the generation of ROS such as toxic gases, ionizing radiation smoking cigarettes, etc. Therefore, ROS along with various types of free radicals are responsible for chronic inflammation that leads to the development and progression of various diseases. Various aspects of immunological and inflammatory responses are primarily responsible for inflammation (Phaniendra *et al.*, 2015). Pro-inflammatory cells are frequently an important source of several inflammatory mediators such as cytokines (TNF-α, IL-1, and IL-6) and ROS, which either directly or indirectly aid in the development of various diseases like cancer, diabetes, aging, cardiac dysfunction (atherosclerosis and hypertension), rheumatoid arthritis, neurodegenerative disorders (Parkinson's disease, Alzheimer's disease, and multiple sclerosis), cataracts and respiratory ailments (Phaniendra *et al.*, 2015). Plants are long been utilized as the basis of many traditional medicines exerting protective effects against several diseases due to their antioxidative properties (Patel *et al.*, 2014). Therefore, antioxidants derived from natural sources, including plant materials, are becoming more and more important because it has been shown that these chemicals are essential for the regular upkeep of cellular functions as well as overall health and well-being. Thus, increasing the consumption of antioxidants which have the ability to scavenge free radicals might be a safer and more effective way to combat illnesses (Wolfe *et al.*, 2008). In recent decades, an increasing number of researches have concentrated on plant extracts that include antioxidant properties that may lower the chance of acquiring chronic diseases. The bleeding heart vine, or bag flower, is a beautiful decorative plant used in the floriculture industry. It belongs to the family Lamiaceae and the genus *Clerodendrum* (Patel *et al.*, 2014). In Asia, Australia, Africa, and America, *Clerodendrum thomsoniae* is widely spread (Shrivastava & Patel, 2007). It is used as a folk remedy by traditional healers of Cameroon to treat diabetes and obesity. According to Shrivastava and Patel (2007), the plant is also used as medication in Indian and Japanese traditional systems to cure a number of serious illnesses, including cancer, typhoid, syphilis, jaundice, and hypertension. *C. thomsoniae* is claimed to have a variety of ethnomedicinal uses, however, there is not enough data to support these claims. The background information and limitations drove us to execute the study using *C. thomsoniae*. Therefore, an initiative was undertaken to evaluate the free radical scavenging activity of *C. thomsoniae* leaf extract (CT) using different *in vitro* antioxidant methods, justifying its beneficial effects on oxidative stress. In addition, anti-inflammatory and cytotoxicity of CT were measured to evaluate possible cytotoxic mechanisms of *C. thomsoniae*. Gas chromatography-mass spectroscopy (GC-MS) was further employed to identify the putative compounds. Based on the ethnomedicinal importance of CT in various diseases, we eventually designed an *in silico* molecular docking to find out the binding pattern between the identified compounds of CT and inflammation and cancer proteins, asserting the probable anti-inflammatory and anti-cancer functions of CT.

MATERIALS AND METHODS

Collection and Extraction of *Clerodendrum thomsoniae*

Leaves of *C. thomsoniae* were collected in January 2024 from Shivmandir, Siliguri, West Bengal (26.712° N, 88.366° E). Fresh *C. thomsoniae* leaves (CT) that had been air-dried for three weeks and free of disease were ground into a fine powder using a mechanical grinder. Adopting the soxhlation process, 10 g of crushed leaves were extracted in 70% methanol (v/v) for 7 h. The extract was concentrated using a rotary evaporator. The extract was then lyophilized to create a dry powder that could be used later.

Determination of *in vitro* Antioxidant Activity

Nitric oxide (NO) radical scavenging assay

The quantification technique of the Griess-I-Llosvoy reaction at physiological pH (Garratt, 2012) was used to measure the nitric oxide radical scavenging activity with minor adjustments. Briefly, phosphate-buffered saline (pH 7.4), sodium nitroprusside (SNP; 10 mM), and different concentrations of CT extract (0-200 μg/mL) were mixed and made the final volume of 3 mL. After the mixture was thoroughly vortexed and incubated for 150 mins at 25 °C, 0.5 mL of the pre-incubated reaction mixture was mixed with 1 mL of sulfanilamide (0.33%), which was diluted in 20% glacial acetic acid, and allowed to sit at room temperature for 5 mins. To facilitate color production, 1 mL of N-(1-Naphthyl) ethylenediamine dihydrochloride (NEED; 0.1%) was added and the mixture was kept at 25 °C for an additional 30 mins. Using distilled water as a blank, the absorbance was measured at 540 nm. Curcumin functioned as a standard reference. The percent of inhibition was measured according to the following Equation 1:

$$\text{Percentage of scavenging} = \frac{A0 - A1}{A0} \times 100 \tag{1}$$

Where, A0=absorbance of the control and A1=absorbance in the presence of samples and standard.

The concentration that inhibited NO radical by 50% was taken as the IC_{50} value and this was calculated as per linear regression.

Hydrogen peroxide scavenging assay

The CT extract's hydrogen peroxide (H_2O_2) scavenging capacity was calculated using a modified version of Long *et al.* (1999). H_2O_2 (50 mM) and different concentrations of CT extract (0-200 μg/mL) were combined in a screw-capped bottle, and the mixture was allowed to dark-incubate for 30 mins at room temperature (≈25 °C). Next, 90 μL of H_2O_2, 10 μL of HPLC-grade methanol, and 0.9 mL of FOX reagent (made by combining 9 volumes of 4.4 mM butylated hydroxytoluene in HPLC-grade methanol with 1 volume of 1 mM xylenol orange and 2.56 mM ammonium ferrous sulfate in 0.25 M H_2SO_4) were added. After giving the mixture a gentle vortex and letting it sit for 30 mins, the absorbance at 560 nm was determined. Ascorbic

acid was utilized as a positive control. The percentage inhibition was measured as before using equation I. The concentration that inhibited H_2O_2 radical by 50 % was taken as the IC_{50} value, and this was calculated as per linear regression.

Hydroxyl radical scavenging assay

Hydroxyl radical scavenging activity of the CT extract was conducted using the Fenton reaction model (Kunchandy & Rao, 1990) with a small modification. 2-deoxy-2-ribose (2.8 mM), monopotassium phosphate-potassium hydroxide buffer (KH_2PO_4-KOH; 20 mM; pH 7.4), $FeCl_{3}$ (100 μM), ethylene diamine tetraacetic acid (EDTA; 100 μM), hydrogen peroxide (H_2O_2; 1.0 mM), ascorbic acid (100 μM), and varying concentrations of CT extract (0-200 μg/mL) were added to the reaction mixture until a final volume of 1 mL was achieved. After carefully mixing the reaction mixture, it was incubated for 60 mins at 37 °C. Following the completion of the incubation period, the 0.5 mL mixture was carefully transferred into a fresh tube and mixed with 1 mL each of aqueous thiobarbituric acid (TBA; 1%) and trichloroacetic acid (TCA, 2.8%). Once more, the finished mixture was incubated for 15 mins at 90 °C. The absorbance at 532 nm was measured after the mixture had cooled to room temperature in comparison to an appropriate blank solution. A positive control was employed as ascorbic acid. The percentage inhibition was measured as before using Equation 1. The concentration that inhibited hydroxyl radical by 50% was taken as the IC_{50} value, and this was calculated as per linear regression.

Superoxide radical scavenging assay

The assay was conducted in accordance with Fontana *et al.* (2001). The nitro-blue tetrazolium (NBT) is reduced to purple formazan in the presence of the nonenzymatic PMS/NADH system, which produces superoxide radicals when exposed to oxygen. Phosphate buffer (20 mM, pH 7.4), NBT (50 μM), PMS (15 μM), NADH (73 μM), and varying doses (0-200 μg/mL) of CT extract were combined to create a reaction mixture (1 mL). After gently vortexing the mixtures, they were incubated for five mins at room temperature. The amount of formazan produced was estimated by measuring the absorbance at 562 nm in comparison to the equivalent blank samples. Quercetin served as a positive reference. The percentage inhibition was measured as before using Equation 1. The concentration that inhibited superoxide radical by 50% was taken as the IC_{50} value, and this was calculated as per linear regression.

GC-MS Analysis

The CT extract was chemically profiled on a Bruker 450 Gas Chromatograph hyphenated to a 300 MS/MS mass spectrometer (GC-MS), according to a standard method by Nodola *et al.* (2024). The GC-MS system comprised an HP-5 MS fused silica capillary system with phenylmethylsiloxane as the stationary phase, operating at 70 eV in an EI mode. The capillary column dimension was 30 m x 0.25 mm (length x internal diameter), with a film thickness of 0.25 μm. The

column's initial temperature was set at 50 °C and heated to 240 °C at the rate of 5 °C/min, while the final temperature was kept at 450 °C for a run time of 66.25 min. Helium was used as the carrier gas at a flow rate of 1.0 mL/min, while the split ratio was 100:1. Scan time was 78 min at a scanning range of 35 to 450 amu. The CT extract (500 mg) was first solubilized in 5 mL of methanol. The filtrate (1 mL) was reconstituted in 300 mL of n-hexane and centrifuged at 12000 rpm for 15 mins. The supernatant (200 μL) was treated with 100 μL of Tris(trimethylsiloxy)(vinyl)silane. Finally, 1 μL of the treated sample was injected for analysis. The GC-MS system was operated at 70 eV in a negative electron ionization (EI) mode. The retention time (RT), and mass-to-charge ratio (*m/z*) of each of the compounds identified in the CT extract were obtained. The major peaks were scanned for the molecular weights of the compounds at *m/z* 40-990.

In vitro Anti-inflammatory Study

The *in vitro* anti-inflammatory property of CT extract was determined by its inhibitory effect on protein denaturation, using the egg albumin denaturation assay (Ameena *et al.*, 2023) with slight modification. A 0.2 mL of albumin from a fresh chicken egg, 2.8 mL of phosphate buffer saline at pH 6.4, and 2 mL of CT extract at 12.5, 25, 50, 100, and 200 μg/mL concentrations, were mixed in three replicates. The reaction mixture was incubated at 37 °C for 15 mins away from direct light. Then, it was boiled at 70 °C for 5 mins in a thermostatic water bath. The resulting mixture was allowed to cool before the absorbance was measured at 655 nm wavelength. Diclofenac was used as the reference anti-inflammatory drug. The percentage inhibitory effect of CT on egg albumin denaturation (EAD) was calculated according to the following Equation 2:

$$\text{Percentage inhibition of EAD} = \frac{A0 - A1}{A0} \times 100 \qquad (2)$$

Where, EAD=egg albumin denaturation, A0=absorbance of the control, and A1=absorbance in the presence of samples and standard. The concentration that inhibited EAD by 50% was taken as the IC_{50} value, and this was calculated as per linear regression.

Cytotoxicity Study

Cell culture

The South African company Highveld Biologicals (Pty) Ltd., located in Lyndhurst, provided the normal (Vero) cell line and the human renal adenocarcinoma (ACHN) cell line. The cells were maintained using Dulbecco's Modified Eagle Medium/ Nutrient Mixture F-12 Ham (DMEM/F12). 10% fetal bovine serum (FBS), 100 mg/mL streptomycin, 100 units/mL penicillin, 0.14% sodium bicarbonate, and 0.1 mM sodium pyruvate were added as supplements. For duration of 24 h, cells were cultured on 35 mm petri dishes at 37 °C, 5% CO_2, and 95% humidity in a CO_2 incubator.

MTT assay

A standard 3-(4,5-dimethylthiazolyl-2)-2,5-diphenyltetrazolium bromide (MTT) test was used to assess cell viability, following Denizot and Lang (1986) instructions. The effects of different doses of CT extract on the inhibition of cancer cell proliferation were examined using the Vero normal cell line and the ACHN human renal adenocarcinoma cell line. The cells were grown to confluence in a DMEM complete medium that was enhanced with 10% FBS and 1% penicillin-streptomycin solution. The medium was kept at 37 °C in an incubator with 5% CO_2 humidity and a humidified environment. Trypsinized and counted exponentially developing cultured cells were sown at a density of 2×10^4 cells/well in a 96-well plate. The cells were treated with escalating doses of CT extract (40, 80, 120, 160, 200 μg/mL) for 48 h following a 24 h period of adherence. Following the above-mentioned conditions of incubation, 10 μL of MTT solution (5 mg/mL) was applied to each well, and the wells were left in the dark for 3 h. After the medium was carefully removed, 50 μL of isopropanol was used to dissolve the formazan that had developed in the wells, and the plates were left on a plate shaker for five mins. The absorbance was determined at 595 nm with an iMarkTM Microplate Absorbance Reader (Bio-Rad, USA). Every experiment was run in four replicates.

In silico Molecular Docking

Preparation and refinement of the protein and ligand structures

Robust molecular docking research was performed on the phytocompounds against inflammation and cancer proteins that are currently considered attractive targets for future therapeutic development. The PDB structures of NF-κβ (PDB ID 4DN5; 2.50 Å resolution) (Liu *et al.*, 2012) and mdm2 (PDB ID 3W69; 1.90 Å resolution) (Miyazaki *et al.*, 2013) were retrieved from the Protein Data Bank (http://www.rcsb.org). The NF-κβ and mdm^2 proteins were in a complex with a native ligand. The associated native ligand and water molecules were removed from the appropriate protein structures using Pymol software prior to analysis. To get ready for docking in AutoDockTools, polar hydrogen atoms, and Kollman charges were added to the protein structures. The concerned phytocompounds were downloaded from the NCBI PubChem (https://pubchem.ncbi.nlm.nih.gov/). The Open Babel Server was then used to transform the downloaded sdf structures into pdb structures (O'Boyle *et al.*, 2011). The ligand structures underwent energy minimization using the Gromos 96 force field after the PRODRG server was used to optimize their energy (Schüttelkopf *et al.*, 2004).

Determination of the active site and molecular docking

The NF-κβ and mdm^2 proteins were in a complex with a native ligand. The active site of the proteins was predicted using the literature (Liu *et al.*, 2012; Miyazaki *et al.*, 2013) and validated through the CASTp 3.0 (Computed Atlas of Surface Topography of Proteins) online server (Binkowski *et al.*, 2003). The processed protein without a native inhibitor was uploaded to the CASTp 3.0 server and the top result from the best 3 potential ligand-binding sites was chosen for docking. The amino acid residues predicted by CASTp 3.0 were then compared with the amino acids in the active site of the native inhibitor-NF-κβ co-crystallized complex and native inhibitor-mdm2 co-crystallized complex. This was done by manually opening the co-crystallized complex in the Discovery studio visualization tool (Kar *et al.*, 2022a, b) to verify the active site. This allowed for the identification of the interacting residues, which were found to be quite similar to those predicted by the CASTp 3.0 server. The Autodock and Autogrid tools integrated with Autodock4 were used to generate grid maps (X; Y; and Z confirmations; Box center and Box dimension) for each atom of the native inhibitor ligand. In order to obtain the X, Y and Z confirmations (Box center and Box dimension) as a potential target site, molecular docking was carried out using the Autodock4. The ligands of interest were molecularly docked at the active binding sites of the relevant proteins utilizing a stiff protein receptor and a flexible ligand docking methodology through the use of a grid-based molecular docking technology (Kar *et al.*, 2021, 2022a, b). A grid box involving the active site residues of the NF-κβ protein was created, with center_x=-8.0, center_y=30.1, center_z=-4.6, size_x=24.0, size_y=15.1, and size_z=18.9. Similarly, a grid box covering the active binding pocket of mdm2 was employed, with center_x=-34.4, center_y=29.1, center_z=-11.1, size_x=15.7, size_y=18.5, and size_z=28.9. After Autodock Vina finished the molecular docking procedure, the docked complexes were visualized using the Discovery Studio visualization tool (Kar *et al.*, 2022a, b).

Validation of docking protocol by redocking

The conformation of the native ligand which was bound to the active site of the protein was identified. In addition, the conformation of the new ligand (α-tocopherol and stigmasterol) bound at the active site of the protein was also identified. The conformation of the native and new ligands was matched through superimposition and the RMSD values were calculated (Joshi *et al.*, 2014; Saleh-e-In *et al.*, 2019).

Statistical Analysis

To compare the activity of CT extract and references, Student's t-Test integrated with the KyPlot program (version 5.0) was used for statistical analysis.

RESULTS AND DISCUSSION

Evaluation of *in vitro* Antioxidant Activity

The result showed that the CT extract is a powerful nitric oxide radical scavenger with an IC_{50} value of 205.7±11.44 μg/mL (Figure 1a). Nitric oxide (NO) produces peroxynitrite ($ONOO^-$), a strong cytotoxic oxidant that has the power to turn healthy cells into malignant ones when it combines with O_2^- in addition to producing ROS (Chaplin, 2010). The nitration of protein tyrosine residues, lipid peroxidation, DNA, and oligonucleosomal fragment destruction are possible
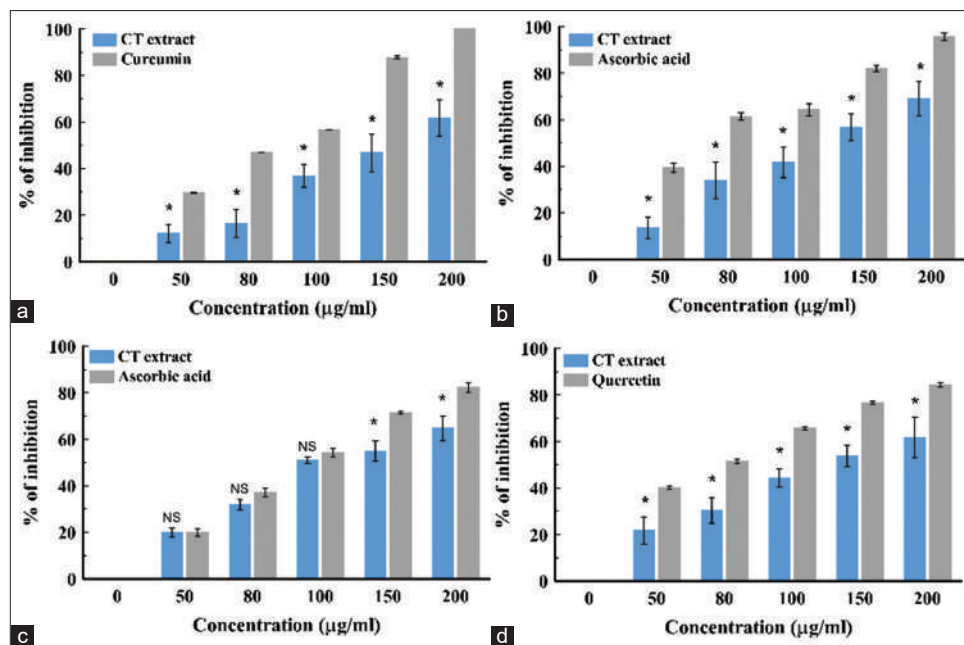
Figure 1: Antioxidant activity of *Clerodendrum thomsoniae* a) Nitric oxide, b) Hydrogen peroxide, c) Hydroxyl radical and d) Superoxide anion (Results are given as mean±S.D (n=3). *$p<0.05$; **$p<0.01$; NS=non-significant)

mechanisms of action for oxidative damage (Hemnani & Parihar, 1998). As a two-electron reductive product of oxygen, hydrogen peroxide (H_2O_2) is commonly considered a harmful agent whose concentration needs to be controlled by the antioxidant system. Merely a mild oxidizing or reducing agent, H_2O_2 is engaged in multiple signal transduction pathways and determines the fate of cells (Lennicke *et al.*, 2015). H_2O_2 is soluble in water, it can readily pass through biological membranes in the presence of transition metal ions, damaging biomolecules including proteins, lipids, and DNA by producing hydroxyl radicals (Chaplin, 2010). According to the results of this investigation, CT extract demonstrated significant hydrogen peroxide scavenging activity with an IC_{50} value of 69.74±6.50 µg/mL (Figure 1b). Remarkably, the CT extract also demonstrated a substantial capacity to scavenge the hydroxyl radical (Figure 1c) and the superoxide anion (Figure 1d). These actions would perfectly complement antioxidant supplements in conjunction with a potent therapeutic intervention involving oxidative stress. Table 1 lists the specific IC_{50} values for each of the corresponding *in vitro* antioxidant assays.

GC-MS Analysis

The GC-MS spectrum of CT extract (Figure 2) showed sixteen major peaks (% composition) with their retention times. The masses of the identified compounds are presented in their molecular ion peaks in the negative mode. The extract was found to be rich in fatty acids, with compounds such as heptadecanoic acid (24.29%), hexadecanoic acid (22.44%), palmitic acid (22.44%), trimethylsilyl ester (20.47%), and linoleic acid (13.44%) among the prominent compounds in the extract. The molecular weights and chemical formula are presented in Table 2. Studies have shown that heptadecanoic acid, α-tocopherol, and stigmasterol are strong antioxidants

Table 1: IC_{50} values of *Clerodendrum thomsoniae* extract and standard for different antioxidant assays

Parameters	CT extract	Standard
Nitric Oxide	205.7±11.44	Curcumin 61.17±0.41
Hydrogen Peroxide	69.74±6.50	Ascorbic acid 48.91±0.12
Hydroxyl Radical	97.81±3.32	Ascorbic acid 92.75±5.91
Superoxide Anion	148.88±9.40	Quercetin 94.5±3.7

Units in µg/mL. Data expressed as mean±S.D (n=3)

and can effectively prevent a number of oxidative stress-related diseases (Yoshida & Niki, 2003; Amarowicz, 2009; Aparna *et al.*, 2012).

Evaluation of *in vitro* Anti-Inflammatory Activity

Protein denaturation has been linked to the occurrence of inflammatory responses that lead to various inflammatory diseases (Osman *et al.*, 2016). Therefore, egg albumin was employed as a model protein in this study to induce denaturation by exposing it to extremes of heat and pH, causing a disruption of its physical characteristics, original chemical conformation, and functional activity (Madhuranga & Samarakoon, 2023). The EAD assay is a fast, reliable, and cost-effective bioassay method that measures the capacity of a substance to prevent or lessen egg albumin denaturation (Goryanin *et al.*, 2022). It was adopted in this study based on the fact that substances having anti-inflammatory properties may be able to stabilize protein structures and prevent denaturation, which is often associated with inflammation and tissue damage. As a result, natural products that significantly decrease the denaturation of egg
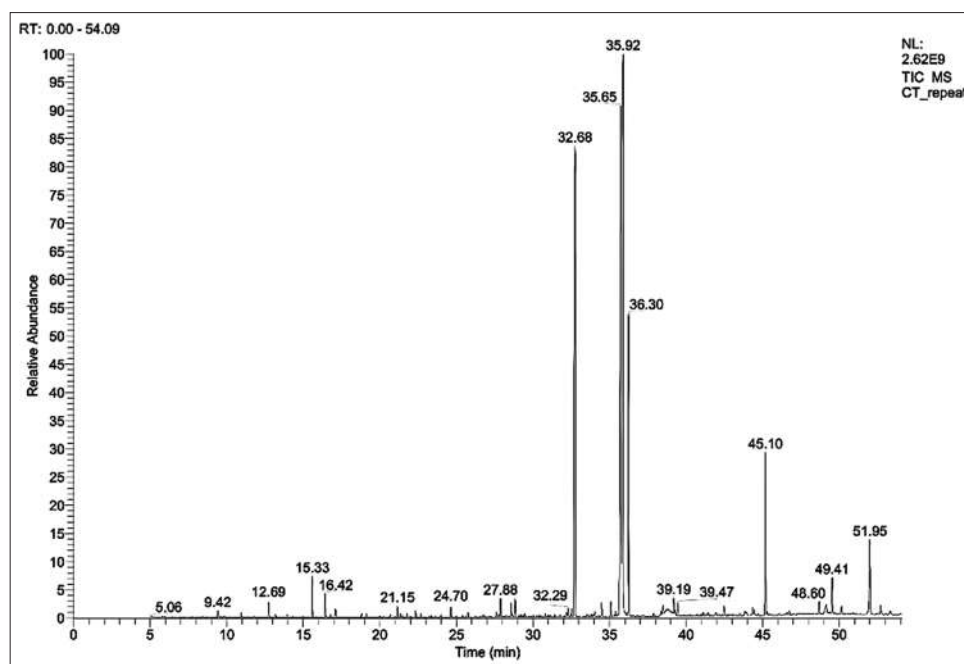
Figure 2: GC-MS chromatogram of CT extract

Table 2: List of phytocompounds identified in *C. thomsoniae* leaf extract by GC-MS analysis

S. No.	RT	Compound name	% Composition	Found Mol Wt[a] (*m/z*)	Theoretical Mol Wt (*m/z*)	Formula
1.	12.69	2-Hexenoic acid	0.61	113.1	114.1	$C_6H_{10}O_2$
2.	15.33	Butanedioic acid	1.85	117.1	118.1	$C_4H_6O_4$
3.	16.42	Glutaric acid	1.11	131.0	132.1	$C_5H_8O_4$
4.	21.15	Dodecanoic acid	0.49	199.2	200.3	$C_{12}H_{24}O_2$
5.	24.70	Azelaic acid	0.37	187.2	188.2	$C_9H_{16}O_4$
6.	27.88	3,7,11,15-tetramethyl 2-Hexadecen-1-ol	0.86	295.4	296.5	$C_{20}H_{40}O$
7.	28.87	Tetradecanoic acid	0.74	227.2	228.4	$C_{14}H_{28}O_2$
8.	32.68	Palmitelaidic acid, trimethylsilyl ester	20.47	327.5	328.6	$C_{19}H_{38}O_2Si$
9.	35.65	Hexadecanoic acid (Palmitic acid)	22.44	255.4	256.5	$C_{16}H_{32}O_2$
10.	35.92	Heptadecanoic acid	24.29	269.5	270.5	$C_{17}H_{34}O_2$
11.	36.30	Linoleic acid	13.44	279.5	280.4	$C_{18}H_{32}O_2$
12.	39.19	Stearic acid	0.86	283.5	284.5	$C_{18}H_{36}O_2$
13.	45.10	Eicosanoic acid	7.02	311.4	312.5	$C_{20}H_{40}O_2$
14.	48.60	Squalene	0.49	409.5	410.7	$C_{30}H_{50}$
15.	49.41	α-Tocopherol	1.60	429.6	430.7	$C_{29}H_{50}O_2$
16.	51.95	Stigmasterol	3.33	411.6	412.7	$C_{29}H_{48}O$

[a]Molecular ion peak read in the negative mode [M-H]-

albumin may be considered potential anti-inflammatory agents (Dharmadeva *et al.*, 2018; Madhuranga & Samarakoon, 2023).

In this study, a concentration-dependent steady increase in the percentage inhibition of EAD was observed for both CT and diclofenac (Figure 3). At 200 µg/mL, CT extract exhibited a similar anti-inflammatory response, with 54.24±4.72% inhibition of EAD, compared to diclofenac, but at a reduced concentration of 50 µg/mL. Furthermore, the inhibitory effects of the extract on EAD were significantly lower than those exhibited by diclofenac at the same concentrations of 25, 50, and 100 µg/mL. Overall, CT extract with an IC_{50} value of 164.59±17.85 µg/mL, possesses a reduced anti-inflammatory activity compared to the reference drug (diclofenac, IC_{50}=48.08±1.64 µg/mL). Although our study findings have shown that diclofenac is more potent as an anti-inflammatory agent than CT extract, there is empirical evidence

alluding to the adverse effects of diclofenac use, which include hepatorenal toxicity and injury in rats (Alabi & Akomolafe, 2020). Conversely, CT extracts have been previously reported to show no visible sign of toxicity (mortality) at 2000 mg/kg b.w. in rodents (Muhammed Ashraf *et al.*, 2021). However, the study further reported that CT extract at 600 mg/kg shows significant elevation of two liver enzymes (SGPT and ALP) in a dose-dependent manner after 28 days, which suggests possible toxicity when administered at a high dose.

Cytotoxicity Assessment by MTT Assay

The CT extract exhibited potent anti-inflammatory and antioxidant properties, prompting additional research for cell viability assays. The MTT test was used to measure the cytotoxicity of the CT extract against the Vero and ACHN cell lines. The two cell lines used in this study, Vero and ACHN,

received similar quantities of the suspension medium in addition to different dosages of CT extract. It is important to note that the extract appeared to be non-cytotoxic to the Vero cell line having demonstrated 78.32±1.19% viability at a concentration of 200 μg/mL with IC$_{50}$ values of 246.34±3.37 μg/mL which reveals the probable safety of this plant (Figure 4a). The CT extract exhibited substantial dose-dependent anti-cancer activity against the ACHN cell line with 33.45±0.66 % viability at a concentration of 200 μg/mL (Figure 4b), with IC$_{50}$ values of 79.03±3.16 μg/mL, after 48 h of treatment. The existence of many phytoconstituents in this plant, the majority of which are soluble in hydro-methanol, may account for the extract's selective cytotoxic activity. Ashraf and colleagues (Muhammed Ashraf *et al.*, 2021) reported that *C. thomsoniae* has significant cytotoxicity, especially for breast cancer cell lines (MCF-7, Hep-G2, A549, HT-29, MOLT-4, Hela), while Changade *et al.* (2024) reported that *C. infortunatum* significantly inhibits cervical cancer. Our findings corroborated these findings.

In silico Molecular Docking

The GC-MS identified CT phytocompounds were used for molecular docking against the NF-κβ and mdm^2 proteins. Table 3 displays the binding energy scores of the phytocompounds
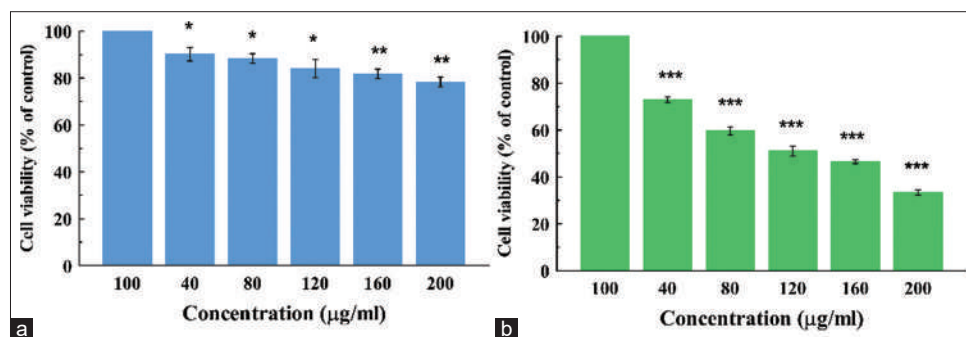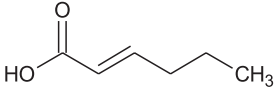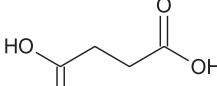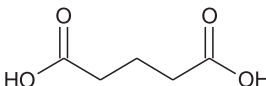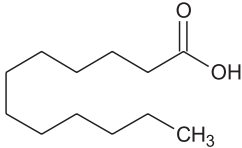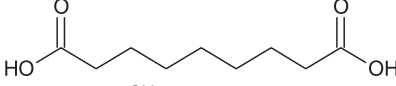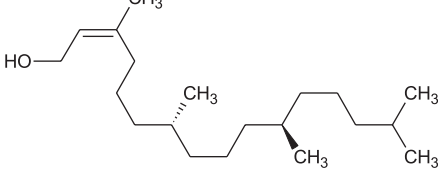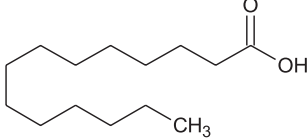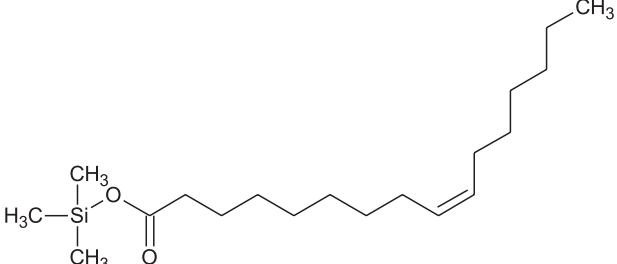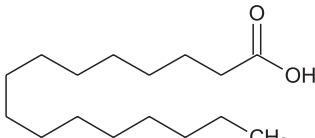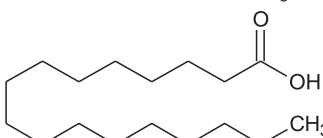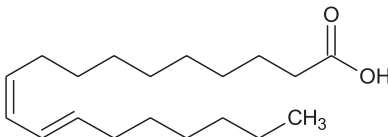
against the NF-κβ protein. The compound α-tocopherol interacts with the hydrophobic interaction (Leu406, Ala427, Met469, Leu471, Lys482, Cys533) and Pi-sigma interactions (Val414 and Leu522) of the protein NF-κβ returning a binding energy score of -9.9 kcal/mol. On the other hand, stigmasterol interaction with NF-κβ (hydrophobic interaction: Val414, Lys482, Cys533) displayed an energy score of -9.4 kcal/mol (Figures 5a & b). Interestingly, the binding potential of α-tocopherol and stigmasterol was significantly higher than that of the suggested inhibitor phosphothio-phosphoric acid-adenylate ester (Table 3) (Liu *et al.*, 2012). It was shown to be associated with residues Leu406, Ala427 (hydrophobic contacts), Gly409, Gly407, Ser476 (hydrogen bonds), Val414, Leu522 (Pi-sigma interactions), and Met469, Asp519 at the active binding pocket of the NF-κβ protein. It's interesting to note that these residues found in the active site are linked to α-tocopherol and stigmasterol, substances that have been demonstrated to play a crucial part in the interaction between NF-κβ and small molecule inhibitors (Figures 5a & b). There are some interesting pharmacological characteristics shown by phytosterols. Ju *et al.* (2010) have reported that α-tocopherol plays a major role in the prevention and inhibition of cancer and suppresses inflammation (Singh & Jialal, 2004; Reiter & Jiang, 2007). Studies have shown that stigmasterol is a strong antioxidant that can help prevent cancer (AmeliMojarad *et al.*, 2022; Wang *et al.*, 2022) and inflammation (Khan *et al.*, 2020; Morgan *et al.*, 2021). Therefore, the presence of α-tocopherol and stigmasterol in CT extract may play a contributory role in the observed *in vitro* anti-inflammatory and anti-cancer activities. Furthermore, fatty acids have been reported to have multiple biological activities such as diabetes, inflammatory, and cardiovascular diseases (Krupa *et al.*, 2024). Linoleic acid (LA) is one of the essential fatty acids that humans need in the diet. Deficiency of LA may lead to growth retardation, infertility, skin, and kidney degeneration, and abrupt changes in the fatty acid composition of lipids (Dobryniewski *et al.*, 2007). Besides, LA has been reported to suppress human tumors (Tsuzuki *et al.*, 2004) and lung tissue cancer. Another metabolite, hexadecenoic acid, and stearic acid have been reported to have a potential protective effect against cancer (Němcová-Fürstová *et al.*, 2019). In addition, squalene was reported as a potent antioxidant as well as beneficial against several carcinogens (Yoshida & Niki, 2003).

Figure 3: *In vitro* anti-inflammatory activity of the leaves of *Clerodendrum thomsoniae*. [Results are given as mean±S.D. (*n* = 3). *p<0.05].

Figure 4: Graphical presentation of cell viability (%) of (a) Vero and (b) ACHN cell lines upon exposure to different concentrations of CT extract for 48 h (Results are given as mean±S.D. (*n* = 4). *p<0.05; **p<0.01; ***p<0.001)
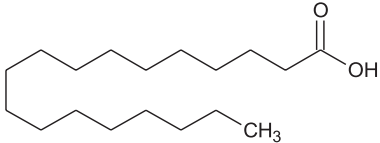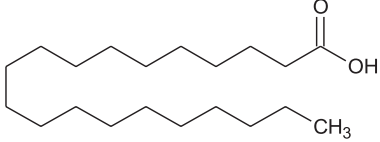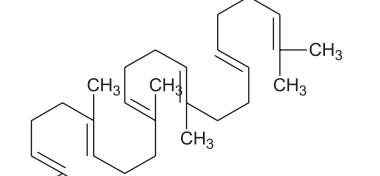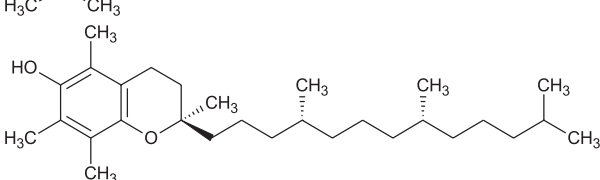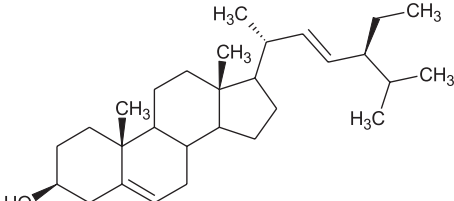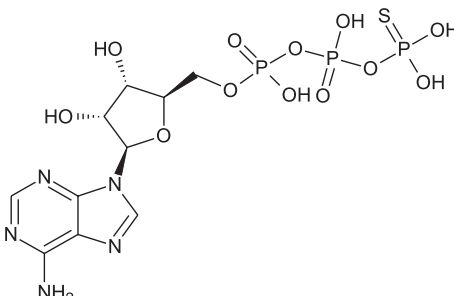
Table 3: Binding energy scores of the phytocompounds in CT extract with NF-κβ protein

Compound name	Chemical structure	Binding energy scores (kcal/mol) NF-κβ (4DN5)
2-Hexenoic acid		-4.2
Butanedioic acid		-4.5
Glutaric acid		-4.6
Dodecanoic acid		-5.2
Azelaic acid		-5.1
3,7,11,15-tetramethyl 2-Hexadecen-1-ol		-5.9
Tetradecanoic acid		-5.5
Palmitelaidic acid, trimethylsilyl ester		-5.9
Hexadecanoic acid (Palmitic acid)		-5.4
Heptadecanoic acid		-5.5
Linoleic acid		-5.5

Table 3: (*Continued*)

Compound name	Chemical structure	Binding energy scores (kcal/mol)
		NF-κβ (4DN5)
Stearic acid		-5.6
Eicosanoic acid		-5.6
Squalene		-5.7
α-Tocopherol		-9.9
Stigmasterol		-9.4
Phosphothiophosphoric acid-adenylate ester (Inhibitor)		-8.0

Chronic inflammation that leads to tumor development, progression, and metastasis is frequently triggered by carcinogenic chemicals, environmental contaminants, UV light, and ionizing radiation. NF-κβ, a transcription factor family that controls various aspects of immunological and inflammatory responses, is primarily responsible for inflammation. It contributes to the production of mRNA that codes for chemokines and pro-inflammatory cytokines (Canli *et al.*, 2017). Pro-inflammatory cells are frequently an important source of several inflammatory mediators that promote tumor growth, such as growth factors, cytokines like TNF-α, IL-1, and IL-6, and reactive oxygen species (ROS), which either directly or indirectly aid in the development of tumors (Schieber & Chandel, 2014). Therefore, inhibiting this protein might be a worthwhile goal for

conditions linked to inflammation (Chan & Yu, 2004). When inflammatory cells (lymphocytes, macrophages, neutrophils, etc.) release cytokines that increase intracellular ROS and RNS in cells, they also trigger BcL-X$_L$, which suppresses the mitochondria-associated multi-domain pro-apoptotic proteins Bak and Bax, ultimately leading to unchecked cell growth and cancer. The examined ligands suppressed the Bcl-X$_L$ protein and increased the production of endonuclease G, cyto-chrome-C, Apoptotic protease activating factor 1 (Apaf-1), Smac/Diablo, Caspase-9, and Caspase-3, all of which are necessary for cell death (Chan & Yu, 2004) (Figure 6).

Table 4 displays the binding energy scores of the phytocompounds against the mdm^2 protein. A binding energy score of -8.7 kcal/mol
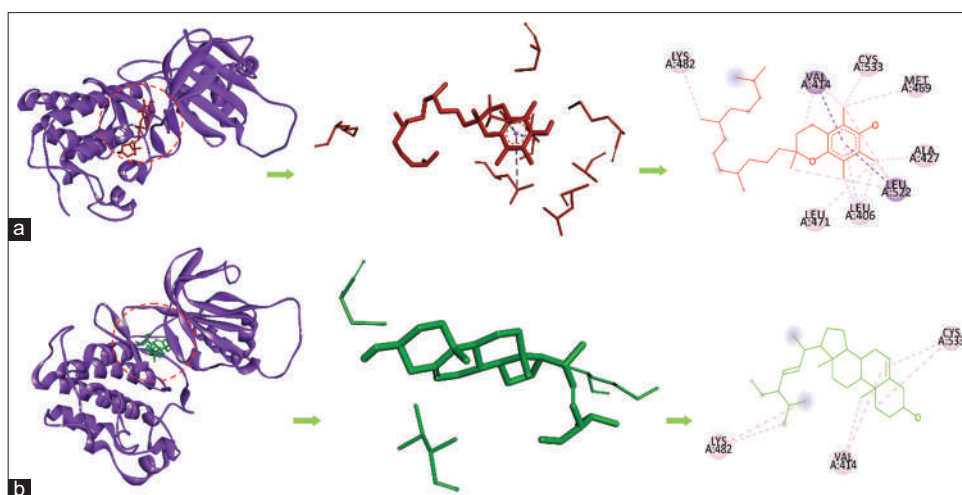
Figure 5: The mode of interaction of a) α-tocopherol, b) stigmasterol with NF-κβ protein. The purple ribbon represents the NF-κβ protein. α-tocopherol and stigmasterol have been illustrated as a red and green stick
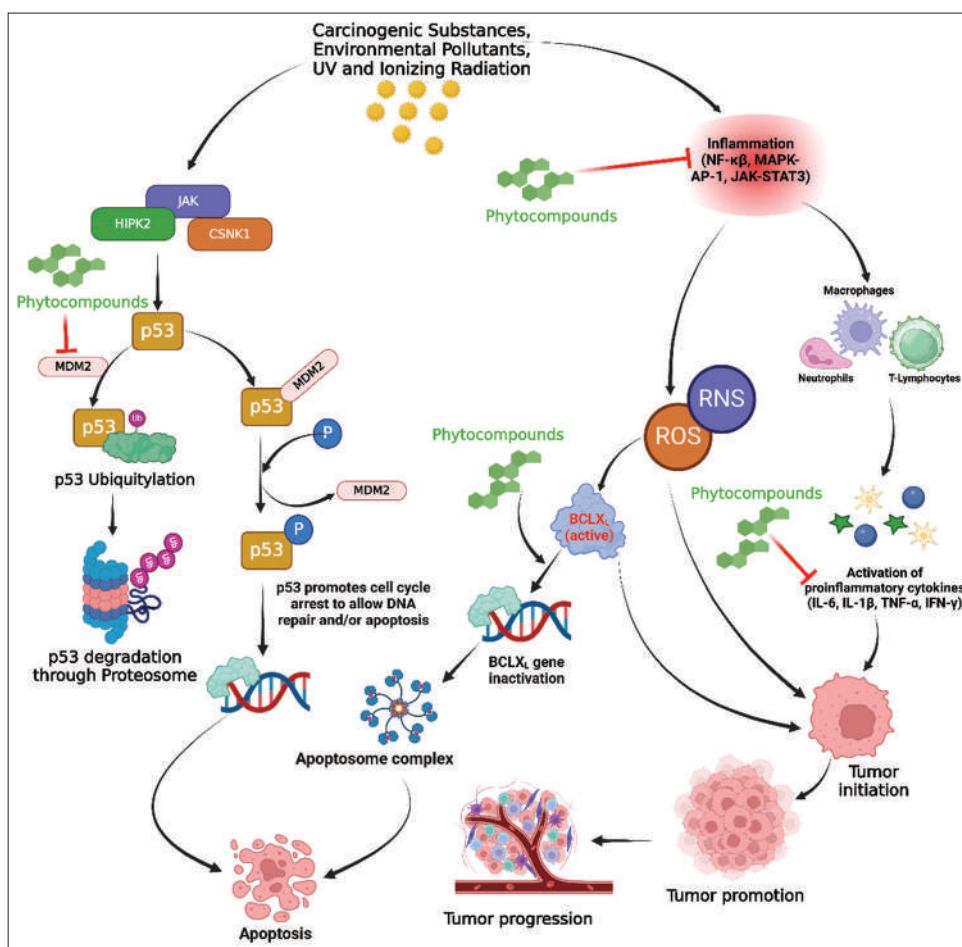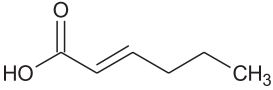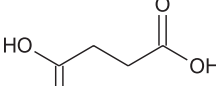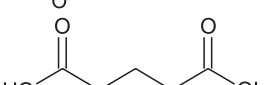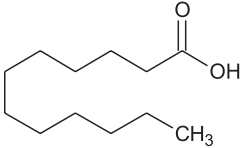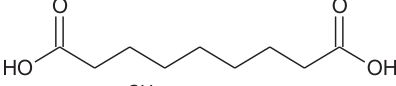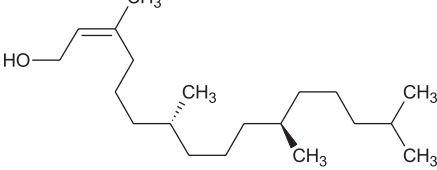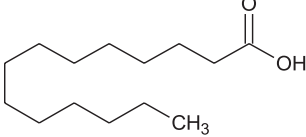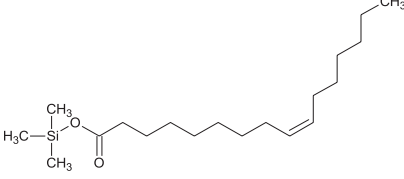

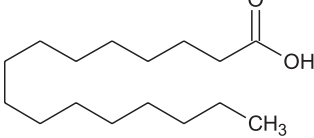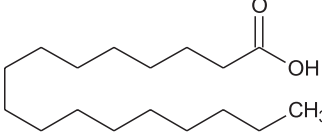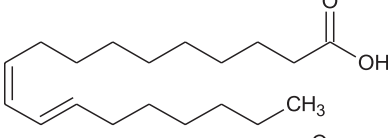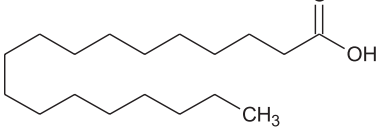**Figure 6:** Schematic representation showing how the phytocompounds from *Clerodendrum thomsoniae* leaf extract plausibly inhibit inflammation and cancer proteins, leading to apoptosis

was seen in the interaction of stigmasterol with the hydrophobic interactions (Leu54, Ile61, Met62, Tyr67, Val75, Phe91, Val93, His96, Ile99) of the mdm2 protein. Whereas, it was evident that hydro-phobic interactions (Leu57, Ile61, Met62, Val93,
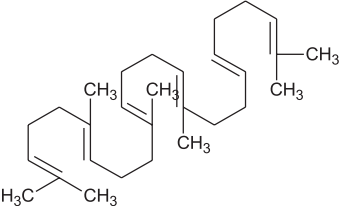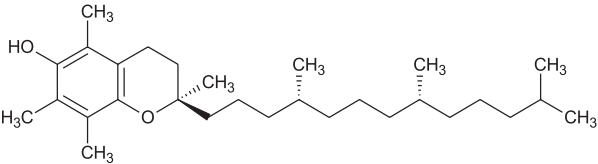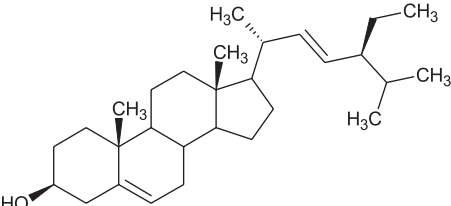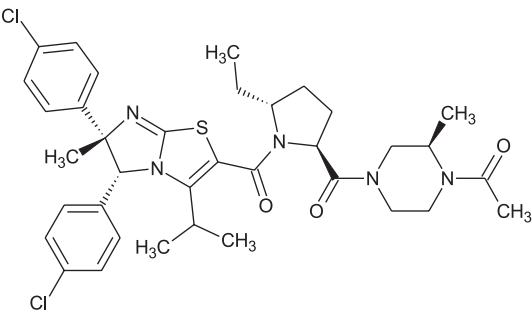
Ile99), hydrogen bond (Tyr100), and Pi-sigma interactions (Leu54 and His96) of the protein mdm² with another compound α-tocopherol returned a binding energy score of -8.2 kcal/mol (Figures 7a & b). Using the proposed inhibitor (5R,6S)-2-

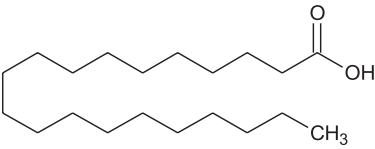## Table 4: Binding energy scores of the phytocompounds with mdm2 protein

Compound name	Chemical structure	Binding energy scores (kcal/mol)
		mdm² (3W69)
2-Hexenoic acid		-4.1
Butanedioic acid		-3.5
Glutaric acid		-3.6
Dodecanoic acid		-4.6
Azelaic acid		-3.8
3,7,11,15-tetramethyl 2-Hexadecen-1-ol		-4.8
Tetradecanoic acid		-4.4
Palmitoleic acid, trimethylsilyl ester		-5.4
Hexadecanoic acid (Palmitic acid)		-4.9
Heptadecanoic acid		-4.6
Linoleic acid		-4.8
Stearic acid		-4.3

Table 4: (*Continued*)

Compound name	Chemical structure	Binding energy scores (kcal/mol)
		mdm^2 (3W69)
Eicosanoic acid		-4.2
Squalene		-5.3
α-Tocopherol		-8.2
Stigmasterol		-8.7
(5R,6S)-2-[((2S,5R)-2-{[(3R)-4-acetyl-3-methylpiperazin-1-yl]carbonyl]-5-ethylpyrrolidin-1-yl) carbonyl]-5,6-bis (4-chlorophenyl)-3-isopropyl-6-methyl-5,6-dihydroimidazo[2,1-b][1,3]thiazole (Inhibitor)		-10.7

[((2S,5R)-2-{[(3R)-4-acetyl-3-methylpiperazin-1-yl]carbonyl}-5-ethylpyrrolidin-1-yl)carbonyl]-5,6-bis(4-chlorophenyl)-3-isopropyl-6-methyl-5,6-dihydroimidazo[2,1-b][1,3]thiazole (Miyazaki *et al.*, 2013), we investigated how the inhibitor bonded to the mdm2 protein and compared its binding pattern to the relevant phytochemicals. The inhibitor exhibited a significant binding potential with a binding energy value of -10.7 kcal/mol. It was shown to be associated with residues Leu54, Ile61, Met62, Tyr67, Gln72, Val75, Val93, Ile99 (hydrophobic contacts), and His96 (π-stakings) at the active binding pocket of the mdm2 protein. Interestingly, Figures 7a and b show that these active site residues are associated with stigmasterol and α-tocopherol, a substance that has been shown to have a significant role in the interaction between mdm2 and small molecule inhibitors (Miyazaki *et al.*, 2013). The MDM2 gene encodes human MDM2, also known as E$_3$ ubiquitin-protein ligase MDM2, which degrades the p53 tumor suppressor by proteasomal means (Mendoza *et al.*, 2014). Here, MDM2 raises the risk

of cancer by acting as a negative regulator on the p53 tumor suppressor gene. Through its binding to tumor suppressors, degradation of cell-cycle inhibitors, and induction of genomic abnormalities, MDM2 stimulates both genomic instability and cell proliferation. Moreover, it binds and breaks down Rb directly, preventing Rb-E2F1 interaction (Schieber & Chandel, 2014). In our study, the considered ligands inhibited mdm2 protein these reliefs p53 from the suppressing effect leading to cell cycle arrest to allow DNA repair and/or apoptosis (Figure 6).

Redocking, Superimposition, and RMSD Calculation

Redocking was performed to validate the docking protocol. It was interesting to note that the NF-κβ protein's native conformation and the re-docked conformation of phosphothio-phosphoric acid-adenylate ester (native ligand) with NF-κβ protein produced the same hydrogen bonds (Gly409), Pi-Alkyl (Leu406, Ala427), Pi-Sulfur (Met469), Pi-
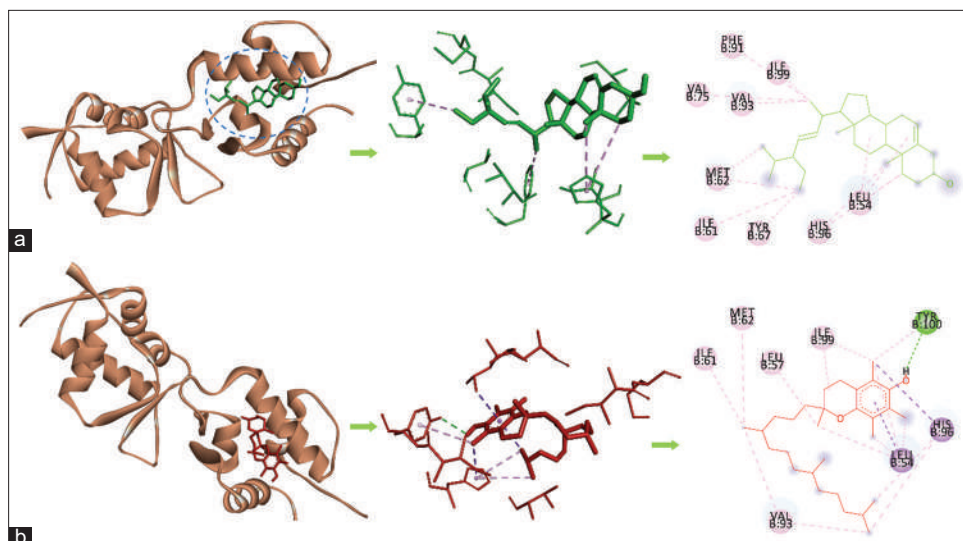
Figure 7: The mode of interaction of a) stigmasterol, b) α-tocopherol with mdm² protein. The brown ribbon represents the mdm² protein. Stigmasterol and α-tocopherol have been illustrated as a green and red stick.
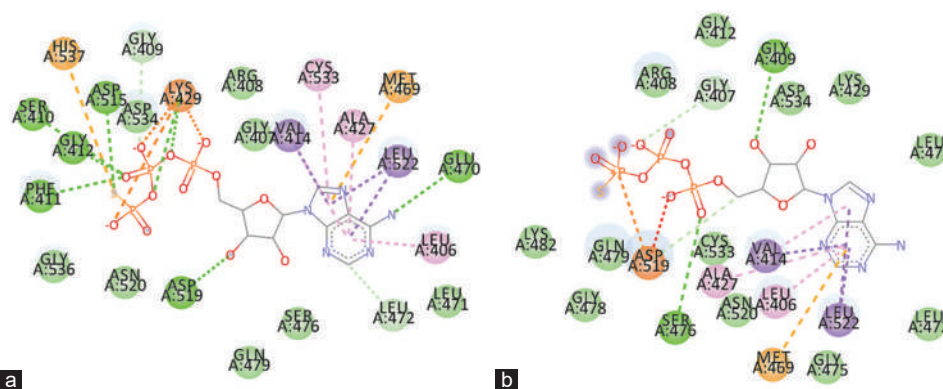

Figure 8: Validation of docking protocol a) NF-κβ protein's co-crystal structure native conformation and b) Re-docked with co-crystal structure's native inhibitor ligand with NF-κβ protein.

Sigma (Val414, Leu522), hydrophobic interactions (Arg408, Asp534, Asn520, Gln479, Leu471) (Figures 8a & b). On the other hand, mdm2 native conformation and the native ligand re-docked with mdm2 protein produced exactly the same Pi-Alkyl bonds (Leu54, Ile61, Tyr67, Val75, Val93, Ile99), hydrophobic interactions (Gly58, Gln72) (Figures 9a & b). The docking program could be employed because of the reproducibility of significant interactions. This demonstrated the docking protocol's effectiveness and legitimacy (Joshi *et al.*, 2014).

It was found that the docked complex (α-tocopherol-NF-κβ, stigmasterol-NF-κβ, and α-tocopherol-mdm², stigmasterol-mdm²) was superimposed completely onto the native co-crystallized NF-κβ and mdm² protein complex without any adjustments. The atoms of amino acids of both the complexes (α-tocopherol-NF-κβ: Leu406, Leu471, Leu522, Ala427, Met469, Cys533, Val414, and stigmasterol-NF-κβ: Cys533, Val414) were superimposed with the native co-crystallized NF-κβ protein without any constraints. Conversely, the amino acid atoms of both the complexes (stigmasterol-

mdm²: Leu54, Ile61, Met62, Tyr67, Val75, Phe91, Val93, His96, Ile99 and α-tocopherol-mdm²: Leu54, Leu57, Ile61, Met62, Val93, His96, Ile99, Tyr100) were likewise overlaid with the native co-crystallized mdm² protein. Figures 10a, b, 11a and b display the superimposed images of the co-crystal structure's native ligand and the re-docked ligands (α-tocopherol, stigmasterol) (Yanuar *et al.*, 2018; Gentile *et al.*, 2020). The findings suggest that the phytocompounds α-tocopherol and stigmasterol, also precisely bind to the amino acids found in the active site cleft of the NF-κβ and mdm² proteins. To confirm the stability of the docked chemicals in biological systems, the average RMSD descriptor for each was computed (Mahmud *et al.*, 2020; Kousar *et al.*, 2020). The fact that the mean average RMSD value of all the complexes is less than the 2 Å stated threshold for RMSD calculation gives us evidence that our docking procedure is valid. Using NF-κβ protein, α-tocopherol and stigmasterol produced RMSD values of 0.50 Å and 0.05 Å, respectively. In contrast, the mdm2 protein containing α-tocopherol and stigmasterol displayed RMSD values of 1.23 Å and 0.09 Å (López-Camacho *et al.*, 2016; Modi *et al.*, 2019).
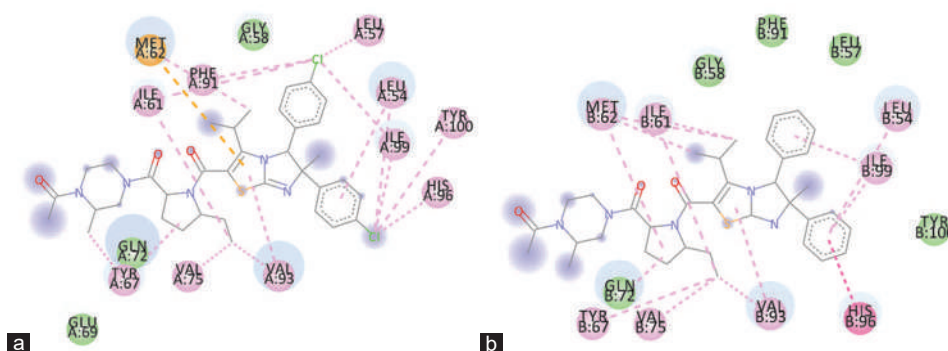
Figure 9: Validation of docking protocol a) mdm² protein's co-crystal structure native conformation and b) Re-docked with co-crystal structure's native inhibitor ligand with mdm² protein.
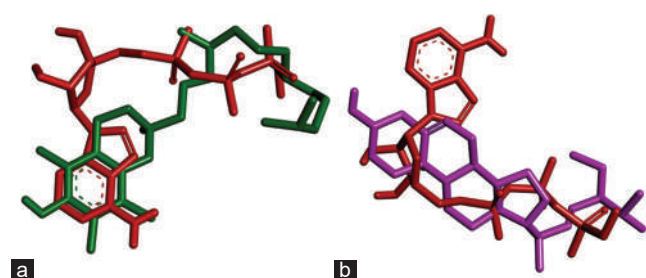

Figure 10: a) Redocked ligand α-tocopherol (green) superimpose to native ligand (red) and b) Re-docked ligand stigmasterol (pink) superimpose to native ligand (red).
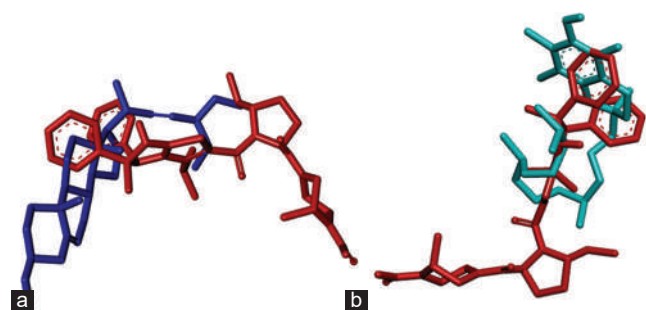

Figure 11: a) Redocked ligand stigmasterol (blue) superimpose to native ligand (red) and b) Re-docked ligand α-tocopherol (sky) superimpose to native ligand (red).

CONCLUSIONS

This study helped to evaluate the antioxidant, anti-inflammatory, and anti-cancer effects of the *C. thomsoniae* extract and identify the putative phytocompounds. The plant extract exhibited significant antioxidant, anti-inflammatory, and anti-cancer activities, indicating the potential medicinal value of the plant. The *in silico* molecular docking results of the putative compounds support the *in vitro* anti-inflammatory and anti-cancer activities of the extract as an inhibitor of the NF-κβ and mdm² proteins and raise the possibility of validating its bioactivity. Further research is warranted to explore the isolation of compounds, their pharmacological properties, bioavailability, safety profile, and potential applications in the development of novel therapeutic agents using *in vivo* models.

REFERENCES

Alabi, Q. K., & Akomolafe, R. O. (2020). Kolaviron diminishes diclofenac-induced liver and kidney toxicity in wistar rats via suppressing inflammatory events, upregulating antioxidant defenses, and improving hematological indices. *Dose-Response, 18*(1), 1559325819899256. https://doi.org/10.1177/1559325819899256

Amarowicz, R. (2009). Squalene: a natural antioxidant?. *European Journal of Lipid Science and Technology, 111*(5), 411-412. https://doi.org/10.1002/ejlt.200900102

Ameena, M., Arumugham, I. M., Ramalingam, K., & Rajeshkumar, S. (2023). Evaluation of the anti-inflammatory, antimicrobial, antioxidant, and cytotoxic effects of chitosan thiocolchicoside-lauric acid nanogel. *Cureus, 15*(9), e46003. https://doi.org/10.7759/cureus.46003

AmeliMojarad, M., AmeliMojarad, M., & Pourmahdian, A. (2022). The inhibitory role of stigmasterol on tumor growth by inducing apoptosis in Balb/c mouse with spontaneous breast tumor (SMMT). *BMC Pharmacology and Toxicology, 23*, 42. https://doi.org/10.1186/s40360-022-00578-2

Aparna, V., Dileep, K. V., Mandal, P. K., Karthe, P., Sadasivan, C., & Haridas, M. (2012). Anti-inflammatory property of n-hexadecanoic acid: structural evidence and kinetic assessment. *Chemical Biology & Drug Design, 80*(3), 434-439. https://doi.org/10.1111/j.1747-0285.2012.01418.x

Binkowski, T. A., Naghibzadeh, S., & Liang, J. (2003). CASTp: computed atlas of surface topography of proteins. *Nucleic Acids Research, 31*(13), 3352-3355. https://doi.org/10.1093/nar/gkg512

Canli, Ö., Nicolas, A. M., Gupta, J., Finkelmeier, F., Goncharova, O., Pesic, M., Neumann, T., Horst, D., Löwer, M., Sahin, U., & Greten, F. R. (2017). Myeloid cell-derived reactive oxygen species induce epithelial mutagenesis. *Cancer Cell, 32*(6), 869-883. https://doi.org/10.1016/j.ccell.2017.11.004

Chan, S.-L., & Yu, V. C. (2004). Brief review proteins of the bcl-2 family in apoptosis signalling: from mechanistic insights to therapeutic opportunities. *Clinical and Experimental Pharmacology & Physiology, 31*(3), 119-128. https://doi.org/10.1111/j.1440-1681.2004.03975.x

Changade, J. V., Thanvi, H., Raut, C., Chavan, M., Prasad, P., & Ladke, V. S. (2024). *In vitro* Evaluation of Anti-Cancer Potential of Different Solvent Extracts Derived from *Clerodendrum Infortunatum* Linn against Cervical Cancer. *Asian Pacific Journal of Cancer Prevention, 25*(3), 1065-1075. https://doi.org/10.31557/APJCP.2024.25.3.1065

Chaplin, D. D. (2010). Overview of the immune response. *The Journal of Allergy and Clinical Immunology, 125*(2), S3-S23. https://doi.org/10.1016/j.jaci.2009.12.980

Denizot, F., & Lang, R. (1986). Rapid colorimetric assay for cell growth and survival: modifications to the tetrazolium dye procedure giving

improved sensitivity and reliability. *Journal of Immunological Methods, 89*(2), 271-277. https://doi.org/10.1016/0022-1759(86)90368-6

Dharmadeva, S., Galgamuwa, L. S., Prasadinie, C., & Kumarasinghe, N. (2018). *In vitro* anti-inflammatory activity of *Ficus racemosa* L. bark using albumin denaturation method. *AYU (An International Quarterly Journal of Research in Ayurveda), 39*(4), 239-242. https://doi.org/10.4103/ayu.AYU_27_18

Dobryniewski, J., Szajda, S. D., Waszkiewicz, N., & Zwierz, K. (2007). Biology of essential fatty acids (EFA). *Przeglad Lekarski, 64*(2), 91-99.

Fontana, M., Mosca, L., & Rosei, M. A. (2001). Interaction of enkephalins with oxyradicals. *Biochemical Pharmacology, 61*(10), 1253-1257. https://doi.org/10.1016/s0006-2952(01)00565-2

Garratt, D. C. (2012). *The quantitative analysis of drugs*. (3rd ed.). New York, US: Springer. https://doi.org/10.1007/978-1-4613-3380-7

Gentile, D., Patamia, V., Scala, A., Sciortino, M. T., Piperno, A., & Rescifina, A. (2020). Putative inhibitors of SARS-CoV-2 main protease from a library of marine natural products: a virtual screening and molecular modeling study. *Marine Drugs, 18*(4), 225. https://doi.org/10.3390/md18040225

Goryanin, I., Ovchinnikov, L., Vesnin, S., & Ivanov, Y. (2022). Monitoring protein denaturation of egg white using passive microwave radiometry (mwr). *Diagnostics, 12*(6), 1498. https://doi.org/10.3390/diagnostics12061498

Hemnani, T., & Parihar, M. S. (1998). Reactive oxygen species and oxidative DNA damage. *Indian Journal of Physiology and Pharmacology, 42*(4), 440-452.

Hirayama, D., Iida, T., & Nakase, H. (2017). The phagocytic function of macrophage-enforcing innate immunity and tissue homeostasis. *International Journal of Molecular Sciences, 19*(1), 92. https://doi.org/10.3390/ijms19010092

Joshi, A. J., Gadhwal, M. K., & Joshi, U. J. (2014). A combined approach based on 3D pharmacophore and docking for identification of new aurora A kinase inhibitors. *Medicinal Chemistry Research, 23*, 1414-1436. https://doi.org/10.1007/s00044-013-0747-5

Ju, J., Picinich, S. C., Yang, Z., Zhao, Y., Suh, N., Kong, A.-N., & Yang, C. S. (2010). Cancer-preventive activities of tocopherols and tocotrienols. *Carcinogenesis, 31*(4), 533-542. https://doi.org/10.1093/carcin/bgp205

Kar, P., Kumar, V., Vellingiri, B., Sen, A., Jaishee, N., Anandraj, A., Malhotra, H., Bhattacharya, S., Mukhopadhyay, S., Kinoshita, M., Govindasamy, V., Roy, A., Naidoo, D., & Subramaniam, M. D. (2022a). Anisotine and amarogentin as promising inhibitory candidates against SARS-CoV-2 proteins: a computational investigation. *Journal of Biomolecular Structure & Dynamics, 40*(10), 4532-4542. https://doi.org/10.1080/07391102.2020.1860133

Kar, P., Saleh-E-In, M. M., Jaishee, N., Anandraj, A., Kormuth, E., Vellingiri, B., Angione, C., Rahman, P. K. S. M., Pillay, S., Sen A., Naidoo, D., Roy, A., & Choi, Y. E. (2022b). Computational profiling of natural compounds as promising inhibitors against the spike proteins of SARS-CoV-2 wild-type and the variants of concern, viral cell-entry process, and cytokine storm in COVID-19. *Journal of Cellular Biochemistry, 123*(5), 964-986. https://doi.org/10.1002/jcb.30243

Kar, P., Sharma, N. R., Singh, B., Sen, A., & Roy, A. (2021). Natural compounds from *Clerodendrum* spp. as possible therapeutic candidates against SARS-CoV-2: An *in silico* investigation. *Journal of Biomolecular Structure and Dynamics, 39*(13), 4774-4785. https://doi.org/10.1080/07391102.2020.1780947

Khan, M. A., Sarwar, A. H. M. G., Rahat, R., Ahmed, R. S., & Umar, S. (2020). Stigmasterol protects rats from collagen induced arthritis by inhibiting proinflammatory cytokines. *International Immunopharmacology, 85*, 106642. https://doi.org/10.1016/j.intimp.2020.106642

Kousar, K., Majeed, A., Yasmin, F., Hussain, W., & Rasool, N. (2020). Phytochemicals from Selective Plants Have Promising Potential against SARS-CoV-2: Investigation and Corroboration through Molecular Docking, MD Simulations, and Quantum Computations. *BioMed Research International, 2020*, 6237160. https://doi.org/10.1155/2020/6237160

Kris-Etherton, P. M., Lichtenstein, A. H., Howard, B. V., Steinberg, D., & Witztum, J. L. (2004). Antioxidant vitamin supplements and cardiovascular disease. *Circulation, 110*(5), 637-641. https://doi.org/10.1161/01.CIR.0000137822.39831.F1

Krupa, K., Fritz, K., & Parmar, M. (2024). Omega-3 Fatty Acids. *StatPearls [Internet].* Treasure Island, FL: StatPearls Publishing.

Kunchandy, E., & Rao, M. N. A. (1990). Oxygen radical scavenging activity of curcumin. *International Journal of Pharmaceutics, 58*(3), 237-240. https://doi.org/10.1016/0378-5173(90)90201-E

Lennicke, C., Rahn, J., Lichtenfels, R., Wessjohann, L. A., & Seliger, B. (2015). Hydrogen peroxide–production, fate and role in redox signaling of tumor cells. *Cell Communication and Signaling, 13*, 1-19. https://doi.org/10.1186/s12964-015-0118-6

Liu, J., Sudom, A., Min, X., Cao, Z., Gao, X., Ayres, M., Lee, F., Cao, P., Johnstone, S., Plotnikova, O., Walker, N., Chen, G., & Wang, Z. (2012). Structure of the nuclear factor κB-inducing kinase (NIK) kinase domain reveals a constitutively active conformation. *Journal of Biological Chemistry, 287*(33), 27326-27334. https://doi.org/10.1074/jbc.M112.366658

Long, L. H., Evans, P. J., & Halliwell, B. (1999). Hydrogen peroxide in human urine: implications for antioxidant defense and redox regulation. *Biochemical and Biophysical Research Communications, 262*(3), 605-609. https://doi.org/10.1006/bbrc.1999.1263

López-Camacho, E., García-Godoy, M. J., García-Nieto, J., Nebro, A. J., & Aldana-Montes, J. F. (2016). A new multi-objective approach for molecular docking based on RMSD and binding energy. In M. Botón-Fernández, C. Martín-Vide, S. Santander-Jiménez, M. A. Vega-Rodríguez (Eds.), *Algorithms for Computational Biology: Third International Conference, AlCoB 2016, Trujillo, Spain, June 21-22, 2016, Proceedings 3* (Vol. 9702, pp. 65-77) Cham, Switzerland: Springer. https://doi.org/10.1007/978-3-319-38827-4_6

Madhuranga, H. D. T., & Samarakoon, D. N. A. W. (2023). *In vitro* Anti-Inflammatory Egg Albumin Denaturation Assay: An Enhanced Approach. *Journal of Natural & Ayurvedic Medicine, 7*(3), 000411. https://doi.org/10.23880/jonam-16000410

Mahmud, S., Uddin, M. A. R., Zaman, M., Sujon, K. M., Rahman, M. E., Shehab, M. N., Islam, A., Alom, M. W., Amin, A., Akash, A. S., & Saleh, M. A. (2021). Molecular docking and dynamics study of natural compound for potential inhibition of main protease of SARS-CoV-2. *Journal of Biomolecular Structure and Dynamics, 39*(16), 6281-6289. https://doi.org/10.1080/07391102.2020.1796808

Mendoza, M., Mandani, G., & Momand, J. (2014). The MDM2 gene family. *Biomolecular Concepts, 5*(1), 9-19. https://doi.org/10.1515/bmc-2013-0027

Miyazaki, M., Naito, H., Sugimoto, Y., Yoshida, K., Kawato, H., Okayama, T., Shimizu, H., Miyazaki, M., Kitagawa, M., Seki, T., Fukutake, S., Shiose, Y., Aonuma, M., & Soga, T. (2013). Synthesis and evaluation of novel orally active p53–MDM2 interaction inhibitors. *Bioorganic & Medicinal Chemistry, 21*(14), 4319-4331. https://doi.org/10.1016/j.bmc.2013.04.056

Modi, P., Patel, S., & Chhabria, M. T. (2019). Identification of some novel pyrazolo [1, 5-a] pyrimidine derivatives as InhA inhibitors through pharmacophore-based virtual screening and molecular docking. *Journal of Biomolecular Structure and Dynamics, 37*(7), 1736-1749. https://doi.org/10.1080/07391102.2018.1465852

Morgan, L. V., Petry, F., Scatolin, M., de Oliveira, P. V., Alves, B. O., Zilli, G. A. L., Volfe, C. R. B., Oltramari, A. R., de Oliveira, D., Scapinello, J., & Müller, L. G. (2021). Investigation of the anti-inflammatory effects of stigmasterol in mice: insight into its mechanism of action. *Behavioural Pharmacology, 32*(8), 640-651. https://doi.org/10.1097/FBP0000000000000658

Muhammed Ashraf, V. K., Kalaichelvan, V. K., Venkatachalam, V. V., & Ragunathan, R. (2021). Evaluation of in vitro cytotoxic activity of different solvent extracts of *Clerodendrum thomsoniae* Balf. F and its active fractions on different cancer cell lines. *Future Journal of Pharmaceutical Sciences, 7*, 50. https://doi.org/10.1186/s43094-021-00206-6

Němcová-Fürstová, V., Balušíková, K., Halada, P., Pavlíková, N., Šrámek, J., & Kovář, J. (2019). Stearate-Induced Apoptosis in Human Pancreatic β-Cells is Associated with Changes in Membrane Protein Expression and These Changes are Inhibited by Oleate. *Proteomics Clinical Applications, 13*(4), 1800104. https://doi.org/10.1002/prca.201800104

Nodola, P., Miya, G. M., Mazwi, V., Oriola, A. O., Oyedeji, O. O., Hosu, Y. S., Kuria, S. K., & Oyedeji, A. O. (2024). *Citrus limon* Wastes from Part of the Eastern Cape Province in South Africa: Medicinal, Sustainable Agricultural, and Bio-Resource Potential. *Molecules, 29*(7), 1675. https://doi.org/10.3390/molecules29071675

O'Boyle, N. M., Banck, M., James, C. A., Morley, C., Vandermeersch, T., & Hutchison, G. R. (2011). Open Babel: An open chemical toolbox. *Journal of Cheminformatics, 3*, 33. https://doi.org/10.1186/1758-2946-3-33

Osman, N. I., Sidik, N. J., Awal, A., Adam, N. A. M., & Rezali, N. I. (2016). *In vitro* xanthine oxidase and albumin denaturation inhibition assay of *Barringtonia racemosa* L. and total phenolic content analysis for potential anti-inflammatory use in gouty arthritis. *Journal of Intercultural Ethnopharmacology, 5*(4), 343.

Patel, J. J., Acharya, S. R., & Acharya, N. S. (2014). *Clerodendrum serratum* (L.) Moon. - A review on traditional uses, phytochemistry and pharmacological activities. *Journal of Ethnopharmacology, 154*(2), 268-285. https://doi.org/10.1016/j.jep.2014.03.071

Phaniendra, A., Jestadi, D. B., & Periyasamy, L. (2015). Free radicals: properties, sources, targets, and their implication in various diseases. *Indian Journal of Clinical Biochemistry, 30*, 11-26. https://doi.org/10.1007/s12291-014-0446-0

Reiter, E., Jiang, Q., & Christen, S. (2007). Anti-inflammatory properties of α-and γ tocopherol. *Molecular Aspects of Medicine, 28*(5-6), 668-691. https://doi.org/10.1016/j.mam.2007.01.003

Saleh-e-In, M. M., Roy, A., Al-Mansur, M. A., Hasan, C. M., Rahim, M. M., Sultana, N., Ahmed, S., Islam, M. R., & van Staden, J. (2019). Isolation and *in silico* prediction of potential drug-like compounds from *Anethum sowa* L. root extracts targeted towards cancer therapy. *Computational Biology and Chemistry, 78*, 242-259. https://doi.org/10.1016/j.compbiolchem.2018.11.025

Schieber, M., & Chandel, N. S. (2014). ROS function in redox signaling and oxidative stress. *Current Biology, 24*(10), R453-R462. https://doi.org/10.1016/j.cub.2014.03.034

Schüttelkopf, A. W., & van Aalten, D. M. F. (2004). PRODRG: a tool for high-throughput crystallography of protein–ligand complexes. *Acta Cryst D: Biological Crystallography, 60*(8), 1355-1363. https://doi.org/10.1107/S0907444904011679

Shrivastava, N., & Patel, T. (2007). *Clerodendrum* and healthcare: an overview. *Medicinal and Aromatic Plant Science and Biotechnology, 1*(1), 142-150.

Singh, U., & Jialal, I. (2004). Anti-inflammatory effects of α-tocopherol. *Annals of the New York Academy of Sciences, 1031*(1), 195-203. https://doi.org/10.1196/annals.1331.019

Tsuzuki, T., Tokuyama, Y., Igarashi, M., & Miyazawa, T. (2004). Tumor growth suppression by α-eleostearic acid, a linolenic acid isomer with a conjugated triene system, via lipid peroxidation. *Carcinogenesis, 25*(8), 1417-1425. https://doi.org/10.1093/carcin/bgh109

Wang, W.-L., Chen, S.-M., Lee, Y.-C., & Chang, W.-W. (2022). Stigmasterol inhibits cancer stem cell activity in endometrial cancer by repressing IGF1R/mTOR/AKT pathway. *Journal of Functional Foods, 99*, 105338. https://doi.org/10.1016/j.jff.2022.105338

Wolfe, K. L., Kang, X., He, X., Dong, M., Zhang, Q., & Liu, R. H. (2008). Cellular antioxidant activity of common fruits. *Journal of Agricultural and Food Chemistry, 56*(18), 8418-8426. https://doi.org/10.1021/jf801381y

Yanuar, A., Pratiwi, I., & Syahdi, R. R. (2018). *In silico* activity analysis of saponins and 2, 5-piperazinedione from marine organism against murine double minute-2 inhibitor and procaspase-3 activator. *Journal of Young Pharmacists, 10*(2s), S16-S19.

Yoshida, Y., & Niki, E. (2003). Antioxidant effects of phytosterol and its components. *Journal of Nutritional Science and Vitaminology, 49*(4), 277-280. https://doi.org/10.3177/jnsv.49.277